

Interareal coupling reduces encoding variability in multi-area models of spatial working memory

Z **e** **P.K.** *****

Department of Mathematics, University of Houston, Houston, TX, USA

E **:** Pe e ac b e ed d . de a ed- e e a a a e
Ruben Moreno-Bote, Foundation
Sant Joan de Deu, Spain

R **:**
Albert Compte, Institut
d'investigacions Biomèdiques
August Pi i Sunyer, Spain
Moritz Helias, Institute for Advanced
Simulation, Germany

***C** **:**
Zachary P. Kilpatrick, Department of
Mathematics, University of
Houston, 651 Phillip G Hoffman Hall,
Houston, 77204-3008 TX, USA
e-mail: zpkilpat@math.uh.edu

$j \neq k$. For $j = 1, 2$, $C_j(x) = c_j$, $C_c(x) = c_c$. $c_c \rightarrow 0$, $c_c \rightarrow (c_1, c_2)$, $c_1 = c_2 = 1$.

MULTIPLE-AREA MODEL OF SPATIAL WORKING MEMORY

N

$$\tau \dot{u}_j(x, t) = -u_j + \varepsilon^{1/2} \sum_{k=1}^N w_{jk} * f(u_k) + \varepsilon^{1/2} W_j(x, t) \quad (6)$$

u_j , $j = 1, \dots, N$. A 10 $w_{jk}(x-y)$ x y k j (E 2). F (E 3) (E 4) H (E 5). A $W_j(x, t)$ $\langle W_j(x, t) \rangle = 0$.

$$\langle W_j(x, t) W_k(y, s) \rangle = C_{jk}(x-y) \delta(t-s), \quad t, s,$$

$j, k = 1, \dots, N$, $j = k$, $j \neq k$. For $C_{ij}(x) = c_{ij}(x)$, $C_{jk}(x) = c_c(x)$, $j \neq k$.

NUMERICAL SIMULATION OF STOCHASTIC DIFFERENTIAL EQUATIONS

(E 1) 10^{-4} 2000 $\langle \Delta_1(t)^2 \rangle$ 5000 Δ_j x j $u_j(x, t)$

RESULTS

(A 1977; C 1998; E

1998). I P O

BUMPS IN THE NOISE-FREE SYSTEM

E (1) $(\varepsilon \rightarrow 0)$. (E 1998; H 1998)



FIGURE 2 | Diffusion of bumps in the dual area stochastic neural field

(Equation 1). (A) $w_{12} = w_{21} = 0$, $w_{11} = w_{22} = 1$, $\sigma = 0.01$, $\theta = 0.5$, $\epsilon = 0.025$. (B) $w_{12} = w_{21} = 0.5$, $w_{11} = w_{22} = 1$, $\sigma = 0.01$, $\theta = 0.5$, $\epsilon = 0.025$.

(Equation 1). (A) $w_{12} = w_{21} = 0$, $w_{11} = w_{22} = 1$, $\sigma = 0.01$, $\theta = 0.5$, $\epsilon = 0.025$. (B) $w_{12} = w_{21} = 0.5$, $w_{11} = w_{22} = 1$, $\sigma = 0.01$, $\theta = 0.5$, $\epsilon = 0.025$.

$$\Phi = (\Phi_1(x, t), \Phi_2(x, t))^T; \mathcal{L} = \begin{pmatrix} -u(x) + w(x) * [f'(U_1(x))u(x)] \\ -v(x) + w(x) * [f'(U_2(x))v(x)] \end{pmatrix}$$

$$\Phi^* = (\Phi_1^*(x, t), \Phi_2^*(x, t))^T; \mathcal{L}^* = \begin{pmatrix} -p(x) + f'(U_1(x))[w(x) * p(x)] \\ -q(x) + f'(U_2(x))[w(x) * q(x)] \end{pmatrix}$$

$$\mathcal{L} = \begin{pmatrix} -u(x) + w(x) * [f'(U_1(x))u(x)] \\ -v(x) + w(x) * [f'(U_2(x))v(x)] \end{pmatrix}$$

$$\mathcal{L}^* = \begin{pmatrix} -p(x) + f'(U_1(x))[w(x) * p(x)] \\ -q(x) + f'(U_2(x))[w(x) * q(x)] \end{pmatrix}$$

$$\mathcal{L} = \begin{pmatrix} -u(x) + w(x) * [f'(U_1(x))u(x)] \\ -v(x) + w(x) * [f'(U_2(x))v(x)] \end{pmatrix} = \begin{pmatrix} -u(x) + w(x) * [f'(U_1(x))u(x)] \\ -v(x) + w(x) * [f'(U_2(x))v(x)] \end{pmatrix} \quad (10)$$

$$\mathcal{L}^* = \begin{pmatrix} -p(x) + f'(U_1(x))[w(x) * p(x)] \\ -q(x) + f'(U_2(x))[w(x) * q(x)] \end{pmatrix} \quad (13)$$

$$\mathcal{L} = \begin{pmatrix} -u(x) + w(x) * [f'(U_1(x))u(x)] \\ -v(x) + w(x) * [f'(U_2(x))v(x)] \end{pmatrix} \quad (12)$$

$$\mathcal{L}^* = \begin{pmatrix} -p(x) + f'(U_1(x))[w(x) * p(x)] \\ -q(x) + f'(U_2(x))[w(x) * q(x)] \end{pmatrix} \quad (13)$$

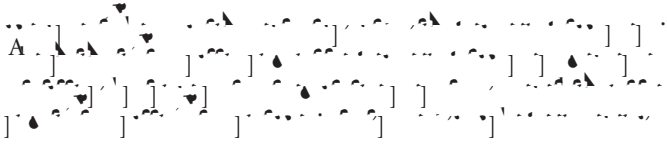
$$f(U_j(x + \Delta_k - \Delta_j)) \approx f(U_j(x)) + f'(U_j(x))U_j'(x) \cdot (\Delta_k - \Delta_j),$$

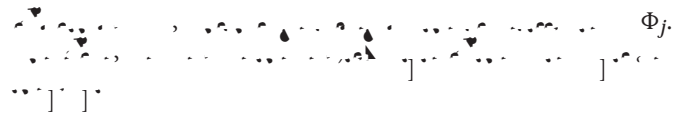
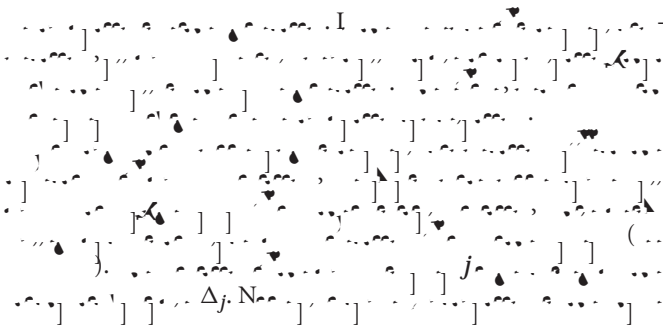
$$\mathcal{L}^* = \begin{pmatrix} -p(x) + f'(U_1(x))[w(x) * p(x)] \\ -q(x) + f'(U_2(x))[w(x) * q(x)] \end{pmatrix} \quad (13)$$

$$j = 1, 2; k \neq j. \quad (12)$$

$$\mathcal{L}^* = \begin{pmatrix} -f'(U_1)U_1' + f'(U_1)[w * [f'(U_1)U_1']] \\ 0 \end{pmatrix} = \mathbf{0}$$

$$\begin{aligned}
 & \text{...} (t) \text{...} E \text{...} (17) \text{...} E \text{...} (19), \\
 & \text{...} t = (-1) \text{...} T \Lambda \text{...} T,
 \end{aligned}$$





$$u_j = U_j(x - \Delta =$$

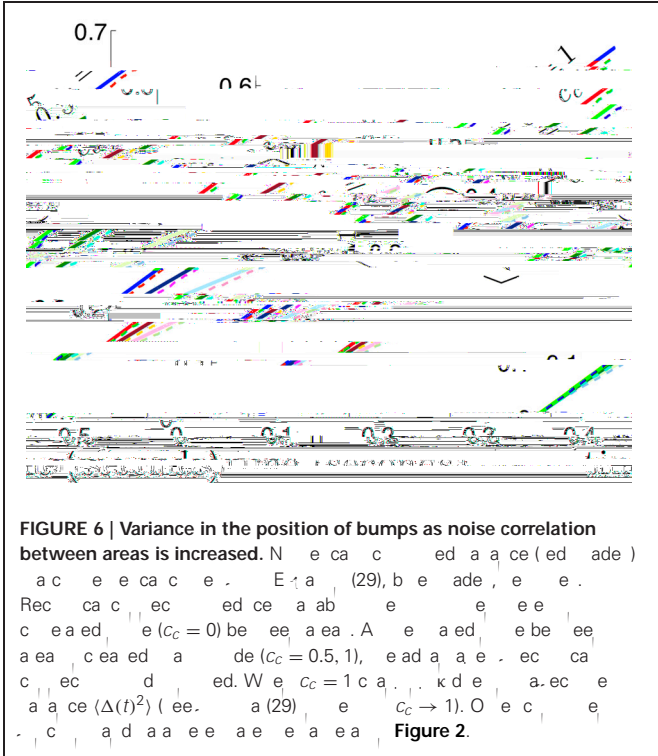


FIGURE 6 | Variance in the position of bumps as noise correlation between areas is increased. The figure shows a series of horizontal plots representing the variance in the position of bumps as noise correlation increases. The plots are labeled with values 0.7, 0.6, 0.5, 0.4, 0.3, 0.2, and 0.1. The plots show a transition from a single bump to multiple bumps as the correlation decreases.

$$\begin{aligned}
 & \text{(E 30)} \\
 & \text{(31)} \\
 & |\Delta_k - \Delta_j| \\
 & j, k \\
 & \text{(31)} \\
 & \mathcal{L}^*
 \end{aligned}$$

$$\int_{-\pi}^{\pi} \Upsilon^T \mathcal{L} \Psi_x = \int_{-\pi}^{\pi} \Psi^T \mathcal{L}^* \Upsilon_x$$

$$\Upsilon = (\Upsilon_1(x), \dots, \Upsilon_N(x))^T$$

$$\mathcal{L}^* \Upsilon = \begin{aligned} & -\Upsilon_1(x) + f'(U_1(x))[w * \Upsilon_1] \end{aligned}$$

$$= \kappa J_N - N\kappa I$$

$$J_N = N \times N \text{ matrix with } I \text{ on the diagonal and } \kappa \text{ elsewhere.}$$

$$\lambda_1 = 0, \lambda_j = -N\kappa \text{ for } j \geq 2, \text{ with } (1, \dots, 1)^T \text{ as an eigenvector for } \lambda_1.$$

$$j = 1, \dots, j$$

- Neurophysiol. 79, 2919–2940. doi: 10.1152/jn.1995.79.11.2919
- Cohen, J. D., Lesh, R. A., Gauthier, G., & Pashler, T. A. (1992). The visual word length effect: A perceptual explanation. *Science* 258, 1498–1501. doi: 10.1126/science.11359647
- Cohen, C. L., Doolittle, J. R., & Gauthier, M. E. (1996). The visual word length effect: A perceptual explanation. *J. Neurophysiol.* 76, 2841–2852. doi: 10.1152/jn.1996.76.6.2841
- Cohen, A., Berman, N., Gauthier, M. E., & Pashler, T. A. (2000). The visual word length effect: A perceptual explanation. *Cereb. Cortex* 10, 910–923. doi: 10.1093/cercor/10.9.910
- Cohen, C. L., & Gauthier, M. E. (2004). A perceptual explanation of the visual word length effect. *Neuroscientist* 10, 553–565. doi: 10.1177/1073858404268742